ELSEVIER

Available online at www.sciencedirect.com

SCIENCE DIRECT®

Applied Mathematical Modelling 30 (2006) 10–37

APPLIED MATHEMATICAL MODELLING

www.elsevier.com/locate/apm

From rooted to floating vegetal species in lagoons as a consequence of the increases of external nutrient load: An analysis by model of the species selection mechanism

Francesco Cioffi *, Francesco Gallerano

Dipartimento di Idraulica, Trasporti e Strade, Universitá degli Studi di Roma 'La Sapienza', Via Eudossiana 18 00184 Rome, Italy

Received 1 March 2002; received in revised form 1 January 2005; accepted 4 March 2005
Available online 4 May 2005

Abstract

In this paper, the substitution mechanism of rooted aquatic plants (as eelgrass) with floating species (as Ulva r.) in lagoons are inquired by using a eutrophication model.

The simulations carried out for the specific case of the Lagoon of Tortolì, in Sardinia (Italy), demonstrate the determinant role played by the increase of external phosphorous loads in the vegetal species selection and offer a possible explanation of the selection mechanism.

Once the maximum accumulation capability of adsorbed phosphorous in sediments is reached, the rate of external phosphorous loads produces an increment in the dissolved phosphorous in the water column; such an increment favours the growth of floating species which inhibit, mainly due to light competition effect, the growth of rooted plants.

In the paper, the serious consequences of such a selection in terms of eutrophication processes and vulnerability of anoxic crises are emphasised.

Keywords: Eutrophication; Mathematical models; Lagoon ecology; Water anoxia

* Corresponding author.
E-mail address: francesco.cioffi@uniroma1.it (F. Cioffi).

0307-904X/$ - see front matter
doi:10.1016/j.apm.2005.03.004

1. Introduction

One of the most evident effects of eutrophication in coastal lagoons is the change, in the long run, in vegetable species with reduction of diversity and prevalence of infesting species; such change is also accompanied by an increase of the summer water anoxia vulnerability of the lagoons.

Recent investigations have shown that a strong correlation exists between the lagoon eutrophication levels, vulnerability to water anoxia and type of dominant vegetable species [1]. Specifically, Izzo and Signorini [1] have found, analysing the data of a great number of Italian lagoons, that coastal lagoons having lower eutrophication levels are mainly colonised by rooted species (as eelgrass), while in highly eutrophic environments different floating species, from macroalgae to microalgae, are dominant.

Among the rooted species the eelgrass (*Zostera marina* L.) is the most diffused and important. Eelgrass (*Zostera marina* L.) is, in fact, a widespread submerged macrophyte growing in coastal areas from Alaska to the Mediterranean Sea. Eelgrass is considered to be a very important species in marine ecosystems. Eelgrass meadows serve as nursery grounds for fish and hiding areas for many aquatic species. It is an indicator for good water conditions as it demands clear water to grow in.

Increasing eutrophication has caused increased growth of epiphytes on eelgrass in many coastal area and lagoons, leading to a severe suppression of the natural extension of eelgrass, mainly reducing their extension depth from several meters to 1–2 m. Literature reports a lot of examples of eelgrass suppression and substitution with other kind of macroalgae: in the shallow areas around the island of Masnedo (Denmark) [2,3]; in the North lake of Tunis [4]; in the Lagoon of Venice [5–9]. In the last case studied in the eighties, macroalgae communities have progressively substituted eelgrass and invaded a large portion of the Venice lagoon, with levels of primary productivity (ranging from 1 to 8.3 mg C/gr dw) for the dominant species *Ulva rigida*. Production was high from early Spring to late Autumn, and the biomass density reached peaks up to about 20 kg/mq. Anoxic crises, followed by a consistent release of hydrogen sulphide, was likely to occur, especially during the summer, under particular hydrodynamic and climatic conditions.

Even if it is evident that the specie substitution is a consequence of eutrophication, an detailed explanation of the sequence of the processes leading to substitution of eelgrass with floating algae (as Ulva r.) is far to be clarified. It is reasonable to think that such species substitution depends also on the different physiology of the vegetal species.

The more evident differences between rooted (as eelgrass) and floating vegetal species concern

- the nutrient assimilation modalities;
- life cycle and organic carbon detritus production.

By and large, the differences between the two vegetal species can be evidenced: rooted plants assimilate phosphorous mainly by root-rhizomes from the interstitial water of the sediment [10–13]; while floating species assimilates dissolved phosphorous in the water column. Also the production of organic detritus is different between the two species. In the case of rooted plants the organic detritus is produced at the end of the life cycle, in Autumn, when leaves fall down, while floating species have a more rapid turn over and therefore the organic production is more uniform during the life cycle (from the end of winter to Autumn).

Unfortunately the mechanisms of species substitution cannot immediately be explained by such difference; furthermore also the possibility to obtain an understanding of this mechanism by means of field data is made complex, because the practical impossibility to have quantitative and qualitative measurements to describe in detail the lagoon trophic evolution in the long run.

For this reason, in this paper the mechanism of substitution of rooted aquatic plants (as *Zostera*) with floating species (as Ulva) in lagoons are inquired by using a eutrophication model. The model is described in detail in [14], where it was applied to assess the effect of different management strategies for the control of eutrophication processes in Fogliano lagoon. However a brief description of the model will be carried out in Section 2.

In this paper the model is applied to the real study case of a lagoon in Sardinia (lagoon of Tortolì), which actually presents a very good trophic state, highly stable, as the extended presence of *Zostera marina* shows.

The original goal of the study was that to verify the effects of an external nutrient increment load on the trophic state of the lagoon in order to increase fishing productivity.

In the course of the study, carried out by model, some aspects concerning the mechanisms of species selection came to the light. Since we believe that such a subject is still far from having a thorough explanation, the paper is mainly focused on the discussion of these mechanisms.

The simulations carried out for the specific case of Lagoon of Tortolì in Sardinia (Italy), demonstrate the determinant role of the increase of the external phosphorous loads in the vegetal species selection and offer a possible explanation for the selection mechanism.

Once the maximum accumulation capability of adsorbed phosphorous in sediments is reached, the rate of phosphorous external loads produces an increment in the dissolved phosphorous in the water column; such an increment favours the growth of floating species which inhibit, mainly due to the light competition effect, the growth of rooted plants.

This paper emphasises the serious consequences of such a selection in terms of eutrophication processes and anoxic crises vulnerability.

2. Model description

The model used in this paper to analyse the mechanism of vegetal species substitution is fundamentally that developed by Cioffi e Gallerano (2001), described in detail in [14, Section 3, pp. 395–403]. In [14] each physical, chemical and biological process, represented in the model and affecting eutrophication of lagoons is discussed in detail on the basis of the current literature. Here, for brevity, we only summarise the main features of such a model underlining its main elements of quality.

As it was stressed in [14], the entire construction of the model is based on the observation, deduced by the analyses of field measurements carried out in numerous lagoons, that there is a strong and complicate cause-effect link between eutrophication trend on the long run and instantaneous conditions leading to summer water anoxia. In fact, growth of high quantity of aquatic vegetation (as a consequence of eutrophication) and summer anoxia, have a mutual relation, because high quantities of vegetation produce proportional organic detritus quantities which accumulates into sediments; the aerobic mineralisation of organic detritus in sediments induces considerable dissolved oxygen consumption; if the oxygen flows from the atmosphere to water column and to sed-

iments, due to the turbulence intensity (depending on the instantaneous lagoon hydrodynamic conditions) are not sufficient to compensate the mineralisation consumption of dissolved oxygen, anoxic conditions are reached in sediments. In such conditions both adsorbed phosphorous and hydrogen sulphide are release into the water column. The first produces an increase in orthophosphate concentration in water which stimulates the further vegetal growth (worsening the eutrophication conditions), while the second, due to the re-oxidation of hydrogen sulphide, accelerates the dissolved oxygen consumption into the water column leading to water anoxia.

The described phenomena, affecting the eutrophication trend on the long term of a lagoon, depend on both the hydrodynamic behaviour of water body (due to lagoon morphology, and to entity of the forcing factors tide and wind), and the characteristics of the dominant vegetal species into the lagoon: life cycle, organic detritus production and nutrient uptake.

The model is constructed in such a way to simulate the eutrophication phenomena on a long run (a decade or more), without giving up to the necessity to capture the instantaneous condition leading to water anoxia. For these reasons in the construction of the model the following points have been taken into account

- the unsteady character of eutrophication processes and the different time scales of the phenomena responsible for eutrophication: multiyear (nutrient from input sources and climate change on long term scale), yearly (vegetal biomass life cycles and seasonal metereological variations on medium term scale), daily (organic matter mineralization, metabolic processes, photosynthesis and respiration), daily metereological variation (tides, wind);
- the effects on eutrophication phenomena of the lagoon hydrodynamism produced by external influences (wind, tide), with particular attention to the quantification of both convective and turbulent transport;
- the role of sediments as sink of oxygen, sink and source of nutrients, and source of hydrogen sulphate (H_2S);
- the effect on the eutrophication of the characteristic of the aquatic vegetal species due to the different modality of organic detritus production and of nutrient uptake;
- the necessity to perform simulations to encompass a period long enough for the lagoon to respond completely to the different external conditions imposed;
- the necessity to construct a feasible and flexible tool which must not be too much onerous from point of view of calculation time and computer memory.

The model, whose sketch is shown in Fig. 1, has two coupled modules: an hydrodynamic module and water quality module.

In order to reduce the dimensionality of the equations of hydrodynamic module and substantially facilitate their solution, the conservation of mass and momentum equation are vertically integrated

$$\frac{\partial \eta}{\partial t} + \frac{\partial (U \cdot H)}{\partial x} + \frac{\partial (V \cdot H)}{\partial y} = 0, \tag{1}$$

$$\frac{\partial U}{\partial t} + \frac{\partial HU^2}{\partial x} + \frac{\partial HUV}{\partial y} - fV = -g\frac{\partial \eta}{\partial x} + \frac{1}{\rho}(\tau_{sx} + \tau_{bs}) + \frac{\partial}{\partial x}\left(v_t H \frac{\partial U}{\partial x}\right) + \frac{\partial}{\partial y}\left(v_t H \frac{\partial U}{\partial y}\right)_x, \tag{2}$$

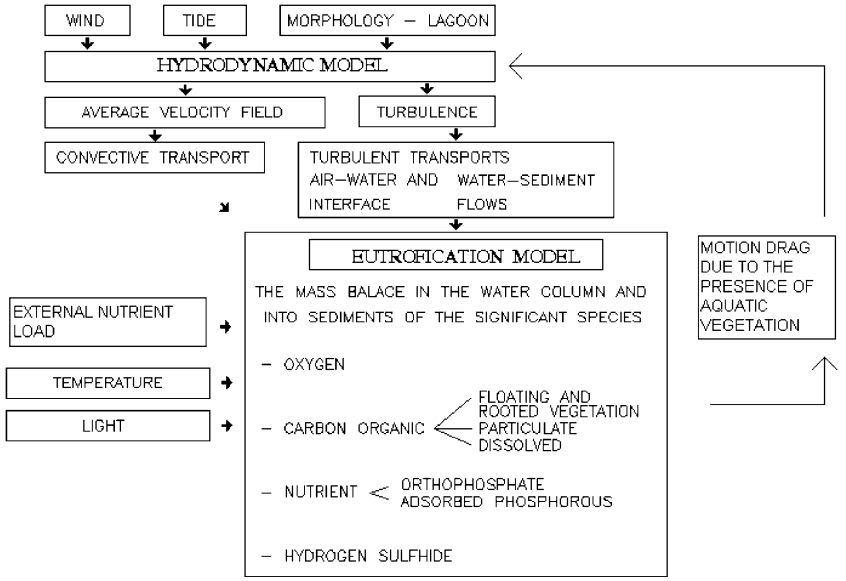

Fig. 1. Sketch of the model.

$$\frac{\partial V}{\partial t}+\frac{\partial HUV}{\partial x}+\frac{\partial HV^2}{\partial y}-fU=-g\frac{\partial \eta}{\partial y}+\frac{1}{\rho}\left(\tau_{sy}+\tau_{by}\right)+\frac{\partial}{\partial x}\left(v_t H\frac{\partial V}{\partial x}\right)+\frac{\partial}{\partial y}\left(v_t H\frac{\partial V}{\partial y}\right)_x, \tag{3}$$

in which U, V are the vertically averaged velocities in the x and y directions respectively, f the Coriolis parameter, η the free surface elevation, H the total water depth, and τ_b and τ_s are, respectively, the bottom and the surface stresses with the subscript indicating the direction. The surface and the bottom stresses are approximated by quadratic formulations in the forcing velocity with a drag and Chezy/Manning coefficient, respectively.

Then the hydrodynamic fields are simulated by solving the two-dimensional vertically average equations. This approach in the case of shallow water lagoon is generally accepted for the simulation of tidal flows; further Hunter and Hearn [15] have demonstrated that -for natural bathymetries and typical values of bottom drag coefficients—this approach can be reasonably followed to simulate the total circulation in the lagoon, also in the case of wind driven flows, being in the most cases the lateral circulation dominant with respect to overturning (vertically varying) circulation.

Due to the importance of turbulent velocity fluctuations into the water column which affect the mass transport phenomena of species, the two-dimensional hydrodynamic module contains a turbulence model for the calculation of turbulent viscosity coefficient.

The turbulent model is described by the following equations:

$$v_t=\frac{C_m K^2}{\varepsilon}, \tag{4}$$

$$\varepsilon=\frac{C_d K^{3/2}}{L_0}, \tag{5}$$

$$\frac{\partial K}{\partial t} - \frac{\partial}{\partial z}\left(v_t \frac{\partial K}{\partial z}\right) - v_t\left[\left(\frac{\partial u}{\partial z}\right)^2 - \left(\frac{\partial v}{\partial z}\right)^2\right] + \varepsilon = 0, \tag{6}$$

in which K is the turbulent kinetic energy per unit volume of velocity fluctuations in the flow, ε the turbulent energy dissipation rate, C_{m} and C_{d} the constants and L_0 is a specific dissipation length scale as reported in [16].

In Eq. (6) it is assumed that the horizontal transport terms are less significant than those along the vertical and that the production of K, represented by the third term on the left, is mainly due to the gradients along the vertical of horizontal velocity components u and v. These gradient may be related to the horizontal stress components τ_{xz} and τ_{yz} by

$$\tau_{xz} = \rho v_t \frac{\partial u}{\partial z} \quad \tau_{yz} = \rho v_t \frac{\partial v}{\partial z}. \tag{7}$$

In the hypothesis of quasi-uniform flow a linear vertical distribution of the stresses may considered

$$\begin{aligned} \tau_{xz} &= S_x - \rho \cdot g \cdot \frac{\partial \eta}{\partial x} \cdot \left(1 - \frac{z}{H}\right), \\ \tau_{yz} &= S_y - \rho \cdot g \cdot \frac{\partial \eta}{\partial y} \cdot \left(1 - \frac{z}{H}\right), \end{aligned} \tag{8}$$

where S_x and S_y are the components of wind stress at the free surface of the lagoon, and H the depth of the water column. The gradients in the second terms on the right-hand side of Eq. (8) are obtained by solving Eqs. (1)–(3).

Then the hydrodynamic module calculates (in each point of the calculation grid) the depth averaged velocity components and the vertical profile of turbulent viscosity coefficient which constitute the inputs of the water quality module.

The water quality module numerically solves the mass balance equations, in the water column and into the sediment layer for each biological, chemical or physical specie affecting eutrophication. In the water column an approach able to represent the three-dimensional character of transport phenomena is considered necessary because the vertical transport of the species—due to turbulence and settling, and the mass flows of the species through the air–water and water–sediment interfaces—plays a determinant role in the evolution of eutrophication processes and development of summer water anoxia, while the horizontal transport phenomena due to the tidal flows affect the water exchanges between sea and lagoon and then control the nutrient accumulation processes in the water body.

In the water quality model the cycling of elements as carbon, nutrients and sulfur in the aquatic system are represented.

The organic carbon is represented in the following forms:

- vegetal organic carbon;
- particulate organic detritus;
- dissolved organic detritus.

Vegetal organic detritus is distinguished in organic carbon contained in vegetable species (mainly phytoplankton or floating macrophytes as Ulva) which utilise dissolved nutrients in the water column, and in organic carbon contained in species provided with a root apparatus, which

benefit from the nutrient directly from sediment (*Zostera*) [10–13]. The vegetal growth, by photosynthesis, is controlled by environmental factor—light, temperature, lagoon hydrodynamics—and by the physiological characteristics of the particular vegetal species.

The mass balance equations for the organic vegetal carbon in the water column are presented in the form:

Algae organic carbon

$$\begin{aligned}&\frac{\partial C_{\mathrm{al}}}{\partial t}+u\frac{\partial C_{\mathrm{al}}}{\partial x}+v\frac{\partial C_{\mathrm{al}}}{\partial y}+w\frac{\partial C_{\mathrm{al}}}{\partial z}\\&\quad=\frac{\partial}{\partial x}\left(v_t\frac{\partial C_{\mathrm{al}}}{\partial x}\right)+\frac{\partial}{\partial y}\left(v_t\frac{\partial C_{\mathrm{al}}}{\partial y}\right)+\frac{\partial}{\partial z}\left(v_t\frac{\partial C_{\mathrm{al}}}{\partial z}\right)\\&\qquad+\left(\mu_{\mathrm{cral}}\cdot f_{\mathrm{a}}(P_{\mathrm{o}})\cdot f_{\mathrm{m}}(I)\cdot f_{\mathrm{al}}(T)-r_{\mathrm{al}}f_{\mathrm{al}}(T)-\frac{K_{\mathrm{d_{al}}}}{f_{\mathrm{al}}(T)}-\frac{K_{\mathrm{p_{al}}}}{f_{\mathrm{al}}(T)}\right)\cdot C_{\mathrm{al}}.\end{aligned}\tag{9}$$

Zostera organic carbon

$$\begin{aligned}&\frac{\mathrm{d}\tilde{C}_{\mathrm{m}}}{\mathrm{d}t}=\int_0^h\left(\mu_{\mathrm{crm}}\cdot f_{\mathrm{s}}(P_{\mathrm{o}},P_{\mathrm{ads}})\cdot f_{\mathrm{m}}(I)\cdot f_{\mathrm{m}}(T)-r_{\mathrm{m}}\cdot f_{\mathrm{m}}(T)-\frac{K_{\mathrm{d_m}}}{f_{\mathrm{m}}(T)}-\frac{K_{\mathrm{p_m}}}{f_{\mathrm{m}}(T)}\right)\cdot C_{\mathrm{m}}\,\mathrm{d}z\\&\tilde{C}_{\mathrm{m}}=\int_0^h C_{\mathrm{m}}(z)\,\mathrm{d}z\quad C_{\mathrm{m}}(z)<C_{\max}.\end{aligned}\tag{10}$$

In Eq. (9), on the left-hand side, the convective transport terms appear; the first three terms on the right-hand side represent the mass turbulent transport; the last term, on the right-hand side, represents the net growth rate of algae (the meaning of symbols is reported in Appendix A). The algae growth is limited by water orthophosphate concentration, light and temperature. In Eq. (9) $f_{\mathrm{a}}(P_{\mathrm{o}}), f_{\mathrm{m}}(I), f_{\mathrm{al}}(T)$ indicate the limiting factors, r_{al} the respiration rate, and $K_{\mathrm{d_{al}}}$, $K_{\mathrm{p_{al}}}$ are, respectively, the particulate and dissolved detritus production rates.

In the simulation of *Zostera* growth phenomena, an approach similar to that proposed in [14] is used; it is assumed that the main nutrient contribution to the vegetation growth of *Zostera* is provided by roots. This hypothesis, in the specific case of the goal of this paper is particularly useful because it allows to distinguish clearly between the floating algae and the rooted plants and thus to analyse the interaction between them. The vegetal growth of *Zostera* is simulated in a process which starts from the bottom of the water column; then the vegetation extends to the upper layers of the water column once a maximum ($C_{\max}$ in Eq. (10), experimentally deduced) vegetal concentration is reached in the lower layers.

In order to represent this growth process the mass balance of the *Zostera* is expressed in integral equation form along the water column depth. In Eq. (10) the terms appear to represent the photosynthetic carbon organic production, the vegetal respiration and the particulate and dissolved organic carbon production rates. The vegetal growth rate of *Zostera* is limited by light, temperature and nutrient concentration into the sediments; phosphorous limitation is expressed by $f_{\mathrm{s}}(P_{\mathrm{o}},P_{\mathrm{ads}})$ where P_{o}, P_{ads} are, respectively, the orthophosphate concentration in the sediment interstitial water and adsorbed phosphorous in the solid phase of sediments. The organic carbon detritus production (both in dissolved or particulate form) is related to the life cycle of the specific

vegetal species present in the lagoon; for floating algae the carbon detritus is continuosly produced during the algae life; for *Zostera* most of the carbon organic detritus is produced at the end of the life cycle, in autumn.

The particulate organic detritus present in water column partly settles and accumulates in sediments; the remain part is transformed, by hydrolysis, in dissolved organic detritus in the water column. The last one is mineralised both in the water column and in sediments by aerobic or anaerobic (in lagoon mainly sulphate reduction) respiration processes.

The mass balance equations in the water column of particulate and dissolved organic carbon are presented in the form

Particulate organic carbon

$$\frac{\partial C_{\mathrm{p}}}{\partial t}+u\frac{\partial C_{\mathrm{p}}}{\partial x}+v\frac{\partial C_{\mathrm{p}}}{\partial y}+(w-v_{\mathrm{s}})\frac{\partial C_{\mathrm{p}}}{\partial z}=\frac{\partial}{\partial x}\left(v_t\frac{\partial C_{\mathrm{p}}}{\partial x}\right)+\frac{\partial}{\partial y}\left(v_t\frac{\partial C_{\mathrm{p}}}{\partial y}\right)+\frac{\partial}{\partial z}\left(v_t\frac{\partial C_{\mathrm{p}}}{\partial z}\right)-K_{\mathrm{p}}C_{\mathrm{p}}+\frac{K_{\mathrm{p_{al}}}}{f_{\mathrm{al}}(T)}\cdot C_{\mathrm{al}}+\frac{K_{\mathrm{p_m}}}{f_{\mathrm{m}}(T)}\cdot C_{\mathrm{m}}. \tag{11}$$

Dissolved organic carbon

$$\frac{\partial C_{\mathrm{d}}}{\partial t}+u\frac{\partial C_{\mathrm{d}}}{\partial x}+v\frac{\partial C_{\mathrm{d}}}{\partial y}+w\frac{\partial C_{\mathrm{d}}}{\partial z}=\frac{\partial}{\partial x}\left(v_t\frac{\partial C_{\mathrm{d}}}{\partial x}\right)+\frac{\partial}{\partial y}\left(v_t\frac{\partial C_{\mathrm{d}}}{\partial y}\right)+\frac{\partial}{\partial z}\left(v_t\frac{\partial C_{\mathrm{d}}}{\partial z}\right)+K_{\mathrm{p}}C_{\mathrm{p}}+\frac{K_{\mathrm{d_{al}}}}{f_{\mathrm{al}}(T)}\cdot C_{\mathrm{al}}+\frac{K_{\mathrm{d_m}}}{f_{\mathrm{m}}(T)}\cdot C_{\mathrm{m}}-\mu_{\mathrm{d}}\cdot f_{\mu}(T)\cdot f(C_{\mathrm{d}})\cdot f(O_2). \tag{12}$$

In Eq. (11), besides the turbulent and convective transports, a term representing the settling (with velocity v_{s}) appears; on the right-hand side in Eq. (11) the fourth term represents the transformation of particulate organic carbon in dissolved carbon, the two following terms are the same which appear in Eqs. (9) and (10), the last term represents the consumption of dissolved organic carbon due to aerobic mineralisation.

In sediments the mass balance equations of particulate and dissolved organic carbon are

Particulate organic carbon

$$\frac{\partial C_{\mathrm{ps}}}{\partial t}=D_{\mathrm{sp}}\frac{\partial^2 C_{\mathrm{ps}}}{\partial z^2}-K_{\mathrm{p}}C_{\mathrm{ps}}. \tag{13}$$

Dissolved organic carbon

$$\frac{\partial C_{\mathrm{ds}}}{\partial t}=D_{\mathrm{ds}}\frac{\partial^2 C_{\mathrm{ds}}}{\partial z^2}+K_{\mathrm{p}}C_{\mathrm{ps}}\frac{1-p_{\mathrm{or}}}{p_{\mathrm{or}}}-K_{\mathrm{s}}C_{\mathrm{ds}}-\mu_{\mathrm{d}}\cdot f_{\mu}(T)\cdot f(C_{\mathrm{ds}})\cdot f(O_2). \tag{14}$$

In Eq. (13) on the right-hand side the terms appear representing, respectively, the dispersion in sediments and the transformation of particulate organic carbon in dissolved organic carbon. The

particulate organic carbon concentration is referred to the sediment solid phase volume, i.e. to the sediment fraction $(1 - p_{or})$ where p_{or} is the porosity.

In Eq. (14), which expresses the dissolved organic carbon consumption due to sulphate reduction in the interstitial water in sediments, on the right-hand side the terms appear representing the dispersion phenomena, the production by hydrolysis, the organic carbon consumption due to sulphate reduction activity and to aerobic mineralisation.

The nutrient simulated in the model is the phosphorus which is represented in the following forms:

- organic phosphorous contained in vegetal biomass and in organic detritus;
- orthophosphate dissolved in water column and into the sediment interstitial water;
- adsorbed phosphorous in sediments.

In the model the mass balance of organic phosphorous is not explicitly made, because it is assumed that phosphorous is present in the biomass and in detritus in a prefixed 1% of organic carbon concentration; then the organic phosphorous mass balance is implicitly obtained by detritus organic carbon (in dissolved and particulate form) and vegetal organic carbon mass balance (Eqs. (9)–(14)).

The mass balance equation of dissolved orthophosphate in the water column is

$$\begin{aligned}\frac{\partial P_o}{\partial t} + u\frac{\partial P_o}{\partial x} + v\frac{\partial P_o}{\partial y} + w\frac{\partial P_o}{\partial z} = {} & \frac{\partial}{\partial x}\left(v_t\frac{\partial P_o}{\partial x}\right) + \frac{\partial}{\partial y}\left(v_t\frac{\partial P_o}{\partial y}\right) + \frac{\partial}{\partial z}\left(v_t\frac{\partial P_o}{\partial z}\right) + K_{p_c}\mu_d \\ & \cdot f_\mu(T)\cdot f(C_d)\cdot f(O_2) - K_{p_c}(\mu_{cral}f_a(P_o)f_m(I)f_{al}(T) \\ & - r_{al}f_{al}(T))\cdot C_{al}. \end{aligned} \tag{15}$$

In Eq. (15) the second last term represents the production of dissolved orthophosphate due to the aerobic mineralisation of dissolved organic matter, the last term represents the consumption of orthophosphate due to the uptake of the floating vegetal species.

The mass balance equation of dissolved orthophosphate in the sediment interstitial water is

$$\begin{aligned}\frac{\partial P_o}{\partial t} = {} & D_{fs}\frac{\partial^2 P_o}{\partial z^2} + K_{p_c}\left(\mu_d\cdot f_\mu(T)\cdot f(C_{ds})\cdot f(O_2) + K_s C_{ds}\right) - \frac{1-p_{or}}{p_{or}}\cdot K_a(P_{ae} - P_a) \\ & + \alpha_p\left(\frac{1-p_{or}}{p_{or}}\right) - \left((\mu_{crm}\cdot f_s(P_o, P_{ads})\cdot f_m(I)\cdot f_m(T)) - f_m(T)\cdot r_m\right)\cdot\frac{\tilde{C}_m K_{pmc}}{h_s}\cdot f'(z). \end{aligned} \tag{16}$$

The first term on the right side represents the dispersion of orthophosphate in sediments, the second term the orthophosphate production due to organic matter mineralisation, in aerobic condition (first term between brackets) and in anaerobic conditions (due to sulphate reduction activity). The last term represents the *Zostera* uptake rate of dissolved orthophosphate and adsorbed phosphorous. This rate is distributed along the vertical in the sediments in proportion to the orthophosphate concentration by the function $f'(z)$.

The third term on the right side of Eq. (16), represents the phosphorous adsorbing-desorption processes in sediments related to the oxygen concentrations. In such a term the adsorbed phos-

phorous concentration P_a and the equilibrium concentration P_{ae} in the sediment solid phase appear.

The mass balance equation of adsorbed phosphorous, in aerobic conditions, is

$$\frac{dP_a}{dt} = K_a(P_{ae} - P_a) - (\mu_{crm} \cdot f_s(P_0, P_a) \cdot f_m(I) \cdot f_m(T) - f_m(T) \cdot r_m) \cdot \frac{\tilde{C}_m K_{pmc}}{h_s} \cdot f''(z), \tag{17}$$

where

$$P_{ae} = P_{max} \frac{P_o}{P_o + K_{po}}$$

while the mass balance equation of adsorbed phosphorous, in anaerobic conditions, is

$$\frac{dP_a}{dt} = -\alpha_p - (\mu_{crm} \cdot f_s(P_0, P_a) \cdot f_m(I) \cdot f_m(T) - f_m(T) \cdot r_m) \cdot \frac{\tilde{C}_m K_{pmc}}{h_s} \cdot f''(z) \tag{18}$$

being P_{max} the maximum concentration of phosphorous that can be adsorbed in the sediment solid phase.

The second term on the right side of Eq. (17) represents the *Zostera* uptake of adsorbed phosphorous by roots. The hypothesis is made that roots can utilise directly the adsorbed phosphorous by enzymatic reactions. Such term is greater than zero when the requirement of phosphorous by roots is greater than the amount of dissolved phosphorous in the sediment interstitial water. The fourth term in Eq. (16) represents the adsorbed phosphorous release in dissolved orthophosphate when anaerobic conditions in sediments are reached; α_p is the desorption rate. In such a condition Eq. (18) holds.

When anaerobic conditions are reached in sediments, the organic matter mineralisation is due to the sulphide reduction activity with hydrogen sulphide production.

The mass balance equation of hydrogen sulphide in the water column is

$$\frac{\partial H}{\partial t} + u\frac{\partial H}{\partial x} + v\frac{\partial H}{\partial y} + w\frac{\partial H}{\partial z} = \frac{\partial}{\partial x}\left(v_t \frac{\partial H}{\partial x}\right) + \frac{\partial}{\partial y}\left(v_t \frac{\partial H}{\partial y}\right) + \frac{\partial}{\partial z}\left(v_t \frac{\partial H}{\partial z}\right) - K_H OH \tag{19}$$

the last term on the right side of Eq. (19) represents the re-oxidation of hydrogen sulphide.

The mass balance equation of hydrogen sulphide in sediments is

$$\frac{\partial H}{\partial t} = D_{fs}\frac{\partial^2 H}{\partial z^2} + \alpha \cdot K_s C_{ds} - K_H OH$$

the second term on the right represents the hydrogen sulphide production in anaerobic conditions; this term is equal to zero for oxygen concentrations less than 1% of oxygen saturation.

As it has been evidenced above, the oxygen concentration has a great influence on the trophic processes: low oxygen concentrations foster, in fact, sulphide reduction activity and phosphorous diffusion from sediments.

The mass balance equation of dissolved oxygen in the water column is

$$\frac{\partial O}{\partial t}+u\frac{\partial O}{\partial x}+v\frac{\partial O}{\partial y}+w\frac{\partial O}{\partial z}=\frac{\partial}{\partial x}\left(v_T\frac{\partial O}{\partial x}\right)+\frac{\partial}{\partial y}\left(v_T\frac{\partial O}{\partial y}\right)+\frac{\partial}{\partial z}\left(v_T\frac{\partial O}{\partial z}\right)$$
$$+\left(\mu_{\mathrm{cral}}\cdot f_{\mathrm{a}}(P_{\mathrm{o}})\cdot f_{\mathrm{m}}(I)\cdot f_{\mathrm{al}}(T)-r_{\mathrm{al}}\cdot f_{\mathrm{al}}(T)-\frac{K_{\mathrm{d_{al}}}}{f_{\mathrm{al}}(T)}-\frac{K_{\mathrm{p_{al}}}}{f_{\mathrm{al}}(T)}\right)\cdot C_{\mathrm{al}}$$
$$+\left(\mu_{\mathrm{crm}}\cdot f_{\mathrm{s}}(P_{\mathrm{o}},P_{\mathrm{a}})\cdot f_{\mathrm{m}}(I)\cdot f_{\mathrm{m}}(T)-r_{\mathrm{m}}\cdot f_{\mathrm{m}}(T)-\frac{K_{\mathrm{d_m}}}{f_{\mathrm{m}}(T)}-\frac{K_{\mathrm{p_m}}}{f_{\mathrm{m}}(T)}\right)$$
$$\cdot C_{\mathrm{m}}-\beta_1\cdot\mu_{\mathrm{d}}f_{\mu}(T)\cdot f(C_{\mathrm{d}})\cdot f(O_2)-\beta_2K_HOH \tag{20}$$

The fourth and fifth terms on the right side represent respectively the net oxygen photosynthetic production due to floating vegetal species and *Zostera* biomass. The sixth term represents the consumption of oxygen for aerobic organic matter mineralisation; the last term the consumption of dissolved oxygen for re-oxidation of hydrogen sulphide.

The mass balance equation of dissolved oxygen in sediments is

$$\frac{\partial O}{\partial t}=D_{\mathrm{fs}}\frac{\partial^2 O}{\partial z^2}-\beta_1\cdot\mu_{\mathrm{al}}f_{\mu}(T)\cdot f(C_{\mathrm{ds}})\cdot f(O_2)-\beta_4\cdot K_H\cdot OH. \tag{21}$$

The second term on the right side represents the consumption of oxygen for organic matter mineralisation; the last term the oxygen consumption for re-oxidation of hydrogen sulphide.

The following relations, expressing the limiting effect of nutrients, temperature, light and oxygen, take part in Eqs. (9)–(21)

$$f_{\mathrm{a}}(P_{\mathrm{o}})=\frac{P_{\mathrm{o}}}{\mathrm{k_{poa}}+\mathrm{P_o}},\quad f_{\mathrm{s}}(P_{\mathrm{o}},P_{\mathrm{a}})=\frac{P_{\mathrm{o}}+P_{\mathrm{a}}}{k_{\mathrm{pos}}+P_{\mathrm{o}}+P_{\mathrm{a}}},\quad f(O_2)=\frac{O}{k_{\mathrm{o}}+O},$$

$$f(C_{\mathrm{d}})=\frac{C_{\mathrm{d}}}{k_{\mathrm{d}}+C_{\mathrm{d}}},\quad f_{\mathrm{m}}(I)=\frac{I}{I_{\mathrm{m}}}\cdot\sin\left(\frac{\pi}{per}\cdot(T-T_{\mathrm{s}})\right)\cdot\mathrm{e}^{-\gamma\cdot h},$$

$$f_{\mathrm{al}}(T)=k_{\mathrm{tal}}^{(T-T_{\mathrm{al}})},\quad f_{\mathrm{m}}(T)=\frac{T}{T_{\mathrm{m}}}\cdot\mathrm{e}^{\left(1-\frac{T}{T_{\mathrm{m}}}\right)},\quad f_{\mu}(T)=k_{t\mu}^{(T-T_{\mu})},$$

being γ calculated by the empirical relation (HR Wallingford Ltd., 1994)

$$\gamma=k_{\gamma1}\cdot(0.025\cdot C_{\mathrm{p}}+0.04)+k_{\gamma2}\cdot C_{\mathrm{a}}+k_{\gamma3}\cdot C_{\mathrm{m}}.$$

The meanings of the symbols used in the appearance, transformation and disappearance terms expressed in Eqs. (9)–(21) are reported in Appendix A.

The boundary conditions which allow the integration of the mass balance equations are

- *at the air–water interface:* conditions of impenetrability are imposed for the dissolved species, except for the oxygen and the hydrogen sulphide, for which it is imposed

$$v_t\frac{\partial O}{\partial z}=-\frac{D_{\mathrm{mo}}}{A_l}\cdot(O_{\mathrm{sat}}-O);\ D_e\frac{\partial H}{\partial z}=-\frac{D_{\mathrm{mh}}}{A_l}\cdot H,$$

where D_{mo} and D_{mh} represent the molecular diffusion coefficients of oxygen and hydrogen sulphide, O_{sat} the saturation concentration of dissolved oxygen, A_l the thickness, variable, of the resistant film at the air–water interface.

- *at the water–sediment interface:* for the dissolved species the equality of concentrations and flows is imposed, while for the C_p the absence of re-suspension is imposed. In the sediment's deepest layers the gradients in vertical direction are assumed equal to zero.

The thickness of the resistant film A_l which appears in boundary conditions at the air water interface, is obtained on the basis of the results of the work of Komori et al. [17], who, elaborating a great number of experimental measurements, have shown that the values of $\frac{K_L}{\sqrt{D \cdot U_{sup}}}$ and the equivalent $\frac{1}{A_l}\sqrt{\frac{D}{U_{sup}}}$ (with $K_L = D/A_l$) are close to 3.0 ($1/m^{1/2}$) and independent of the Reynolds number. D is the molecular diffusivity on the liquid-side (m^2/s), K_L the liquid-side mass transfer coefficient (m/s), U_{sup} is the superficial mean velocity in the proximity of the free surface. The latter is estimated by integrating Eq. (7) with the known value of v_t.

The depth averaged motion equations, Eqs. (1)–(3), the mass balance equations, Eqs. (9)–(21), and the turbulent kinetic energy equation, Eq. (6), are numerically solved by a finite difference scheme (alternate direction implicit technique). In order to take into account the three-dimensional nature of concentration fields of species, the mass balance equations are solved by a splitting technique: (a) the term of mass balance equation representing the rate of local variation in time is splitted in the contribution due to the only convective and turbulent horizontal transport and in that due to the vertical mass transport and the transformation reaction of each species; (b) the former contribution is calculated solving depth averaged mass balance equations; (c) then the calculated rate of local variation in time of the depth averaged concentration is added to the remaining terms of mass balance equation which is numerically integrated along the vertical.

For the Lagoon of Tortolì, which is the specific case examined in this paper, the equations of the hydrodynamic model are numerically integrated on a 50×50 square regular mesh having a space step equal to 50 m (see Fig. 12). This allows to obtain a mesh density able to represent with sufficient detail the velocity current fields inside the lagoon produced by wind and tide. The equations of the water quality model are solved by the above described splitting technique, on the horizontal using the same mesh of hydrodynamic model; along the depth, the water column is divided in 12 equally spaced steps, while in the sediment layer 30 steps, 2 mm high, have been used. Numerical tests have demonstrated that this mesh dimension constitutes a reasonable compromise between the necessity to obtain a detailed description of the hydrodynamic and concentration fields and the necessity to limit the computation time. Because the numerical integration of hydrodynamic equations imposes more stringent time step restrictions than the integration of the water quality model equations, in order to limit the computation time, from a practical point of view, first the hydrodynamic fields are calculated separately and stored; then they are used as input for the water quality model, whose equations can be integrated using a larger time step. Numerical tests have shown that a time step of 300 s can be used for the integration of the water quality model equations without appreciable effects on the solution. In the examined case in order to simulate a period of 10 years on a $50 \times 50 \times 12$ mesh, using a table computer (Pentium IV 1800), the computation time of about 6 h needed.

3. Application

The model, briefly presented in the previous paragraph, has been applied to the Lagoon of Tortolì in Sardinia (Italy) in the location shown in Fig. 2; the goal was to determine the effect of an increase in the external nutrient loads on the trophic behaviour of the lagoon.

The study was set out in the three following phases:

- analysis on the bases of available field measurements of the hydrodynamic and trophic characteristic of the lagoon and calibration of the model;
- simulation by model on long run (10 years) of hydrodynamic and trophic conditions assuming the actual nutrient external loads;
- simulation by model on long run (10 years) of hydrodynamic and trophic conditions hypothesising an increase in nutrient external loads.

3.1. Site description

The Lagoon of Tortolì is shown in Fig. 2 and its main morphological parameter are reported in Table 1.

The depth ranges from a maximum of 4 m, in proximity of Baccasara channel, to a minimum of 1.10 m (see Fig. 4). The lagoon is connected to the sea through two mouths: the first is located at the confluence between Rio Mannu, Baccasara channel (inlet 1 in Fig. 3), the second is south located with respect to the first at the beginning of Baccasara channel (inlet 2 in Fig. 3). A semi-diurnal tide, having a average amplitude equal to 0.30 m, determines the incoming and outgoing tidal flows through the channels.

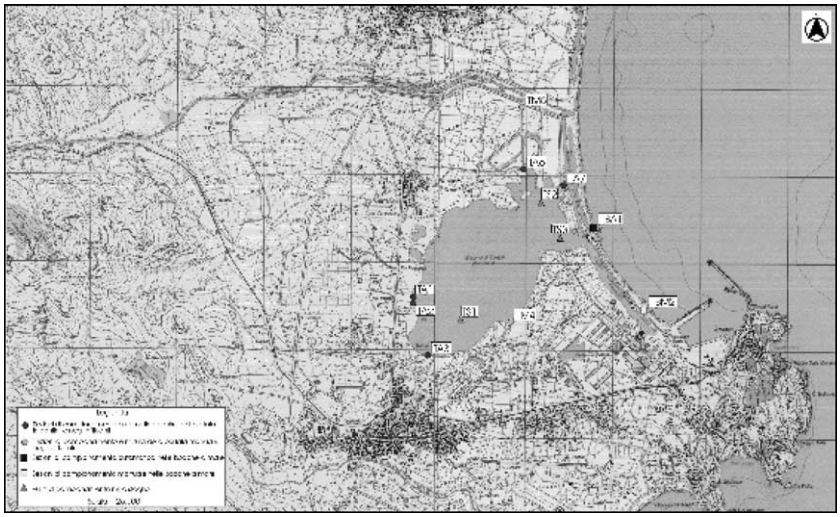

Fig. 2. Lagoon of Tortolì.

Table 1
Main morphometrical parameters of the Lagoon of Tortolì

Area	km^2	2.9
Catchment area	km^2	97
Maximum real length	km	2.5
Maximum real width	km	2.5
Perimeter	km	6

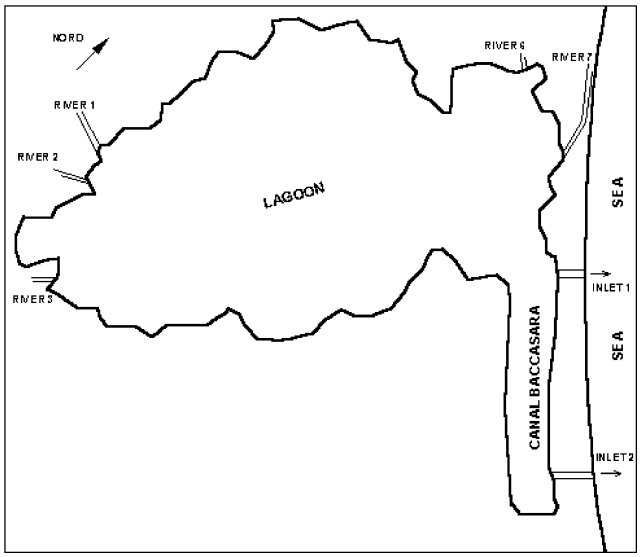

Fig. 3. Inlets of the lagoon.

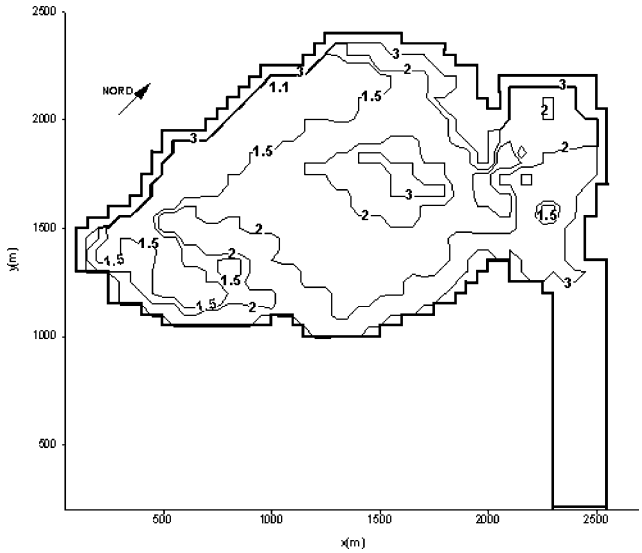

Fig. 4. Bathimetry of the lagoon (m).

The maximum tidal flow rate entering the lagoon from the first mouth (inlet 1) has been estimated by measurements in 3 m^3/s and from the second mouth in 5 m^3/s (inlet 2). Beside tidal flows, the wind blowing over the free surface also influences the lagoon hydrodynamic. Measurements have shown that the most frequent winds are sea breezes blowing along the north-west direction and having a maximum speed of about 3–4 m/s. Along the perimeter of the lagoon there are numerous fresh water inlets, which transport nutrients into the lagoon. The location of the inlets is shown in Fig. 3. Measurements, carried out by hydrocontrol [18] from March 2000 to March 2001, have allowed to estimate the yearly average values of fresh water inflows and external phosphorous loads, which are respectively equal to 0.700 m^3/s and 5.5 tons/years of total phosphorous.

Field measurements of main chemical–physical parameters in three different points in the lagoon, carried out in 2000, have shown that

- the minimum oxygen dissolved, measured at the top and the bottom of the water column, occurs in summer and it is always greater than 4 mg/l (Fig. 5);
- the maximum water temperature peak is reached in summer and does not exceed 25°;
- the dissolved phosphorous concentration in the water column ranges from a maximum value in winter (0.05 mg/l) and a minimum value in summer (0.01 mg/l).

The field observations regarding vegetable species have shown that *Zostera*, is the rooted species which mainly colonised the entire lagoon. The floating species, as fitoplancton and macrophites, are present in minor quantities. The measured concentration of the different vegetal species versus time are shown in Fig. 6.

On the basis of the field measurements available and previously summarised, some conclusions about the actual trophic state of the lagoon can be drawn. The dominant presence of the *Zostera*, the high dissolved oxygen concentration in water column (larger than 4 mg/l) and the low dissolved phosphorous concentration are an indication of a low level of eutrophication of the lagoon.

Since the flushing of nutrients from the lagoon toward the sea is low, as a consequence of the reduced values of tidal flow rates at the inlets, the observed low eutrophication level of the lagoon seems therefore to be due, mainly, to the very low external nutrient loads that enter into the

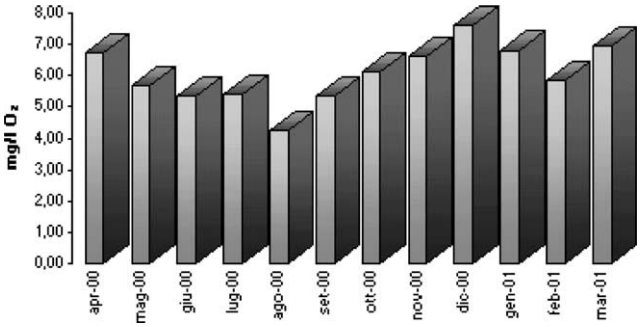

Fig. 5. Measured dissolved oxygen in the water column.

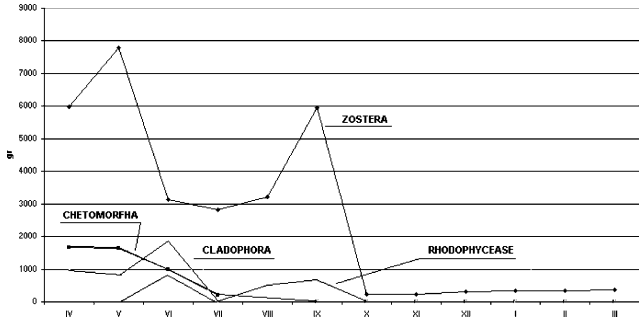

Fig. 6. Measured quantity of the different vegetal species.

lagoon. The effects of an increment of these loads is the object of the simulations by model described in the following pages.

3.2. Simulation results for the actual external loads

Before analysing by model the effect of an increase in external phosphorous load on the trophic state of the lagoon, simulations have were carried out with the actual external loads introduced in the lagoon. The aim was to reach the parameters of the model which allow to fit, by simulations, the actual hydrodynamic and eutrophication behaviour of the lagoon. The measured values of *Zostera* and floating algae biomass, dissolved oxygen and orthophosphate concentration in the water column were taken as a reference. The comparison between the measured and simulated yearly trend of *Zostera* concentration is shown in Fig. 7. The parameter values used in the simulations described in the following are reported in Appendix A.

Hydro-dynamical behaviour of the lagoon induced by tide, in absence and presence of wind was simulated. A gentle breeze having a peak speed equal to 3.5 m/s, which is the more frequent wind condition in the lagoon site, was applied.

In Fig. 8 the hydrodynamic field produced by a incoming tide is shown, as an example, just to highlight that the velocities induced by tide, in absence of wind, are appreciable only in the regions

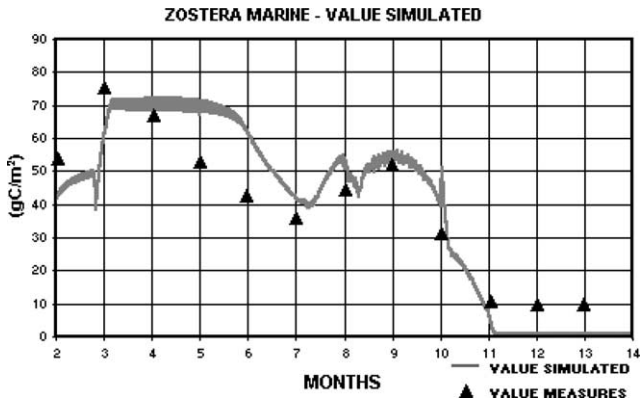

Fig. 7. Comparison between the measured and simulated yearly trend of *Zostera* concentration.

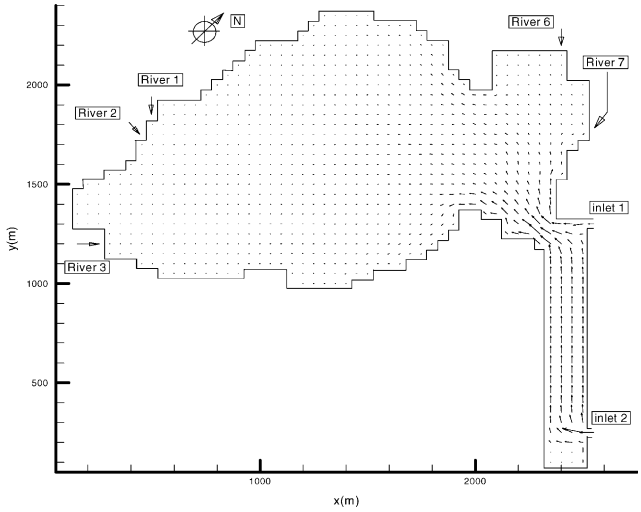

Fig. 8. Hydrodynamic field.

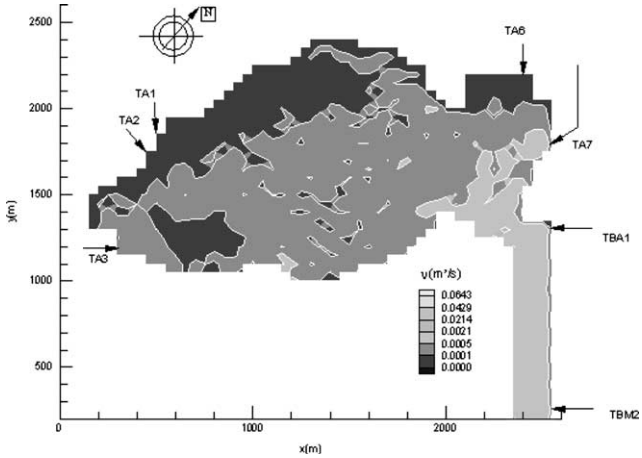

Fig. 9. Turbulence field.

near the mouths, while in the remain part of the lagoon the effect of the tide is practically negligible. This effects is also highlighted in Fig. 9, in which the spatial distribution of turbulent viscosity coefficient corresponding to the previously velocities field is shown. Fig. 9 shows that significant turbulent agitation levels occurs, in absence of wind, only in the region of the lagoon near the mouths connecting the lagoon to the sea.

Despite of the reduced influence of the tidal flows on the current circulation in the lagoon, simulations carried out by the eutrophication model, using the measured external nutrient loads, confirm that the trophic level of the lagoon is actually low and particularly stable. The simulations carried out assuming very critical summer conditions, i.e. a breeze with a 10-day summer stop period, shows, in fact, that the dissolved oxygen concentrations in the water column, in such a critical

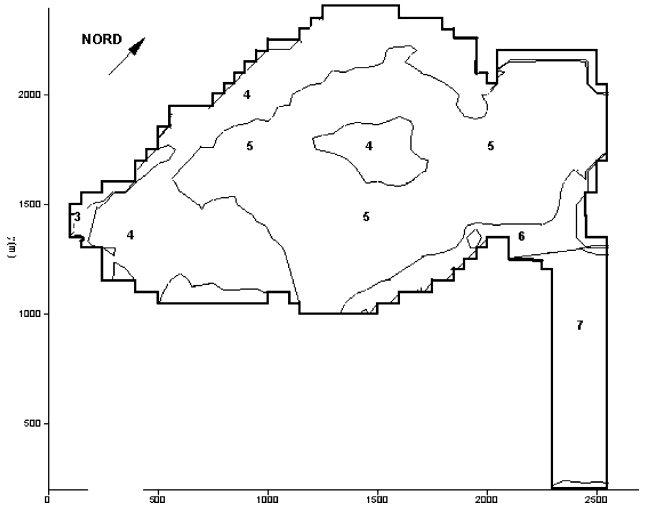

Fig. 10. Dissolved oxygen concentration field during the critical summer period.

period, are greater than 4 mg/l all over the lagoon, as evidenced in Fig. 10 where the dissolved oxygen concentration at the bottom of the water column is shown.

The particularly stable behaviour of the lagoon from a eutrophication point of view can be inferred analysing *Zostera* and floating algae vegetal cycle in the long run (10 years).

The vegetal rooted and floating biomass concentrations versus time in the three points of the lagoon, as indicated in Fig. 12, for a 10-year simulation period are shown in Fig. 11 (right side). Fig. 11 shows that the yearly trend of vegetal biomass remains about the same in each simulated year; just a slight change in the trophic state for point 1 in Fig. 12 can be noted due to a very slow phosphorous accumulation process in the lagoon.

Fig. 11 (right side) and Fig. 13, in which the summer *Zostera* concentration field is also shown, evidence that *Zostera* is the dominant species in the lagoon; the floating algae maximum concentration is in fact remarkably minor than *Zostera* concentrations.

Such substantially stable behaviour of the lagoon is also highlighted in Fig. 11 (left side), where the trend versus time of dissolved oxygen concentration, orthophosphate concentration in the water column and adsorbed phosphorous concentration into the sediments, in the same points of Fig. 12, are shown. In the figure it can be observed that for all the examined points the minimum summer values of dissolved oxygen concentration in the water column, in each point, are higher than 4 mg/l. The values of orthophosphate concentration in the water column are just able to sustain the moderate growth of the floating algae observed. It should also be noted that the adsorbed phosphorous concentration drops to zero in the summer season limiting the growth of *Zostera*.

3.3. Effect of the increase of the external phosphorus load

In this paragraph, the effect of the increase of the external phosphorous loads is analysed starting from the actual lagoon state. The hydrodynamic conditions were the same as those described in the previous paragraph. Two simulation tests were carried out in which respectively

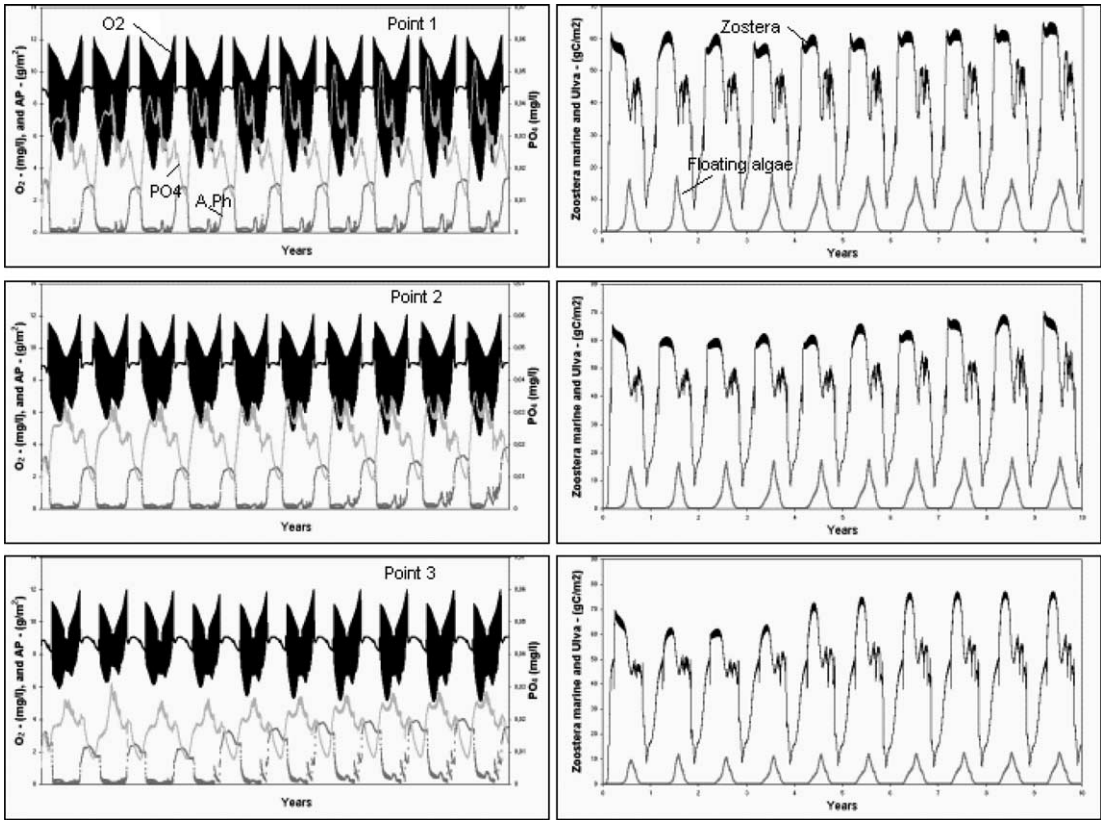

Fig. 11. (Left side) Dissolved oxygen, in the water column; orthophosphate concentration in the water column; adsorbed phosphorous into sediments. (Right side) *Zostera* concentration; floating species concentration.

phosphorous external loads equal to 10 times (configuration a) and 20 times (configuration b) the actual one were applied.

The main effect of the external phosphorous load increment (configuration a) can be inferred from Fig. 14 (right side), in which the *Zostera* and floating algae biomass trend versus time for a 10 year period is shown. The trend is described at the same points of the lagoon in Fig. 12. In point 1, which is far off from the mouths, it can be observed a quite explosive growth of floating algae with respect to rooted plants starting from the forth year of simulation. In the following years, the *Zostera* biomass reduces significantly and at the ninth year it is practically and completely replaced by floating algae.

In point 1, the trend dissolved oxygen concentration in the water column versus time (shown in Fig. 14 (left side)) evidences that once floating algae becomes the dominant vegetal species in the lagoon, summer minimum dissolved oxygen decreases considerably and water anoxia occurs in the long run.

The replacement processes of the vegetal biomass are directly related to the trends versus time of orthophosphate concentration in the water column and adsorbed phosphorous into the sediments, which are shown in Fig. 14 (left side).

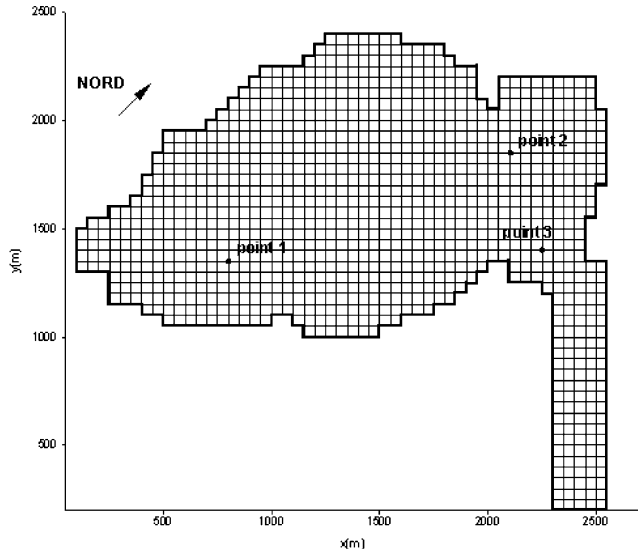

Fig. 12. Points in which the yearly concentration trend of three simulated species is shown.

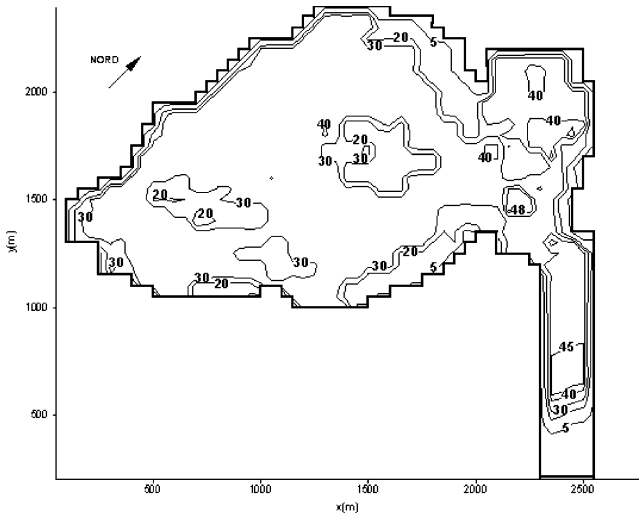

Fig. 13. *Zostera* concentration field.

The figure evidences, as a consequence of the increment of the external load, a progressive increase of adsorbed phosphorous concentration in sediments until it almost reaches the maximum accumulation capability.

Once such maximum capability is reached, also the concentration phosphorous in the water column increases favouring floating species growth. Fig. 14 (left side) shows the presence of summer peaks of orthophosphate concentration in the water column can be observed starting from the forth simulation year. It could be worth to observe that the orthophosphate concentration peaks slightly anticipate the floating algae concentration peaks in the water column.

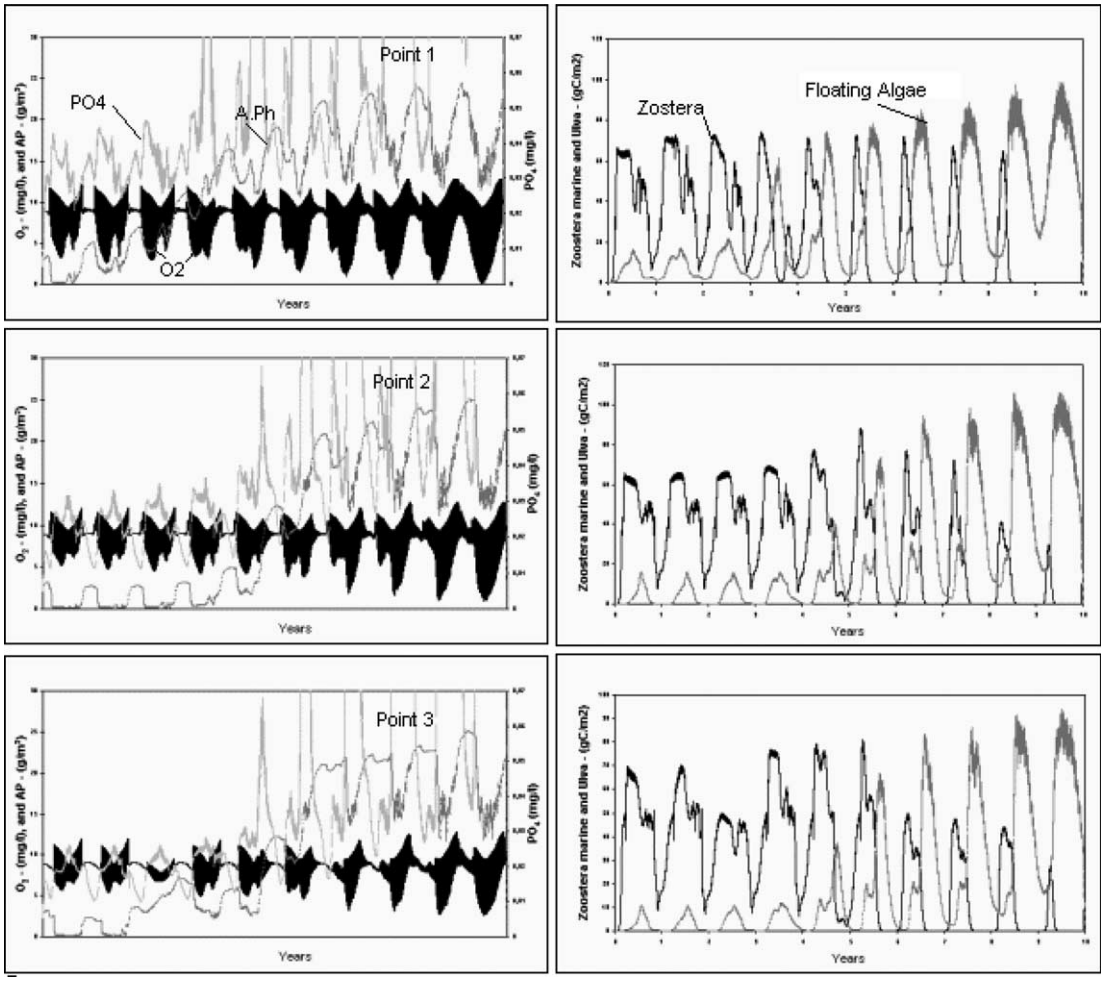

Fig. 14. (Left side) Dissolved oxygen, in the water column; orthophosphate concentration in the water column; adsorbed phosphorous into sediments. (Right side) *Zostera* concentration; floating species concentration.

In points 2 and 3 (see Fig. 12) the concentrations of the different biological and chemical species follow a trend similar to that described above, but the vegetal species replacement occurs more slowly in time. Furthermore the summer minimum dissolved oxygen concentrations are higher than those in points 1 because points 2 and 3 are localised nearer the mouths than point 1, thus the turbulence of the tidal flows allows a better oxygenation of the water column.

The vegetal species substitution does not occur simultaneously in each part of the lagoon, but it progressively extends to the entire lagoon.

In Figs. 15–17 is shown the spatial distribution of dissolved oxygen concentrations in the water column in a summer day (6 a.m) of the fifth simulation year, floating algae and *Zostera* concentrations. It can be observed that the replacement of vegetal species begins in the region far off the mouths where the minor effect of tidal flushing, the lower turbulence levels, the higher organic matter settling and the worst oxygenation conditions of the sediments favour higher orthophos-

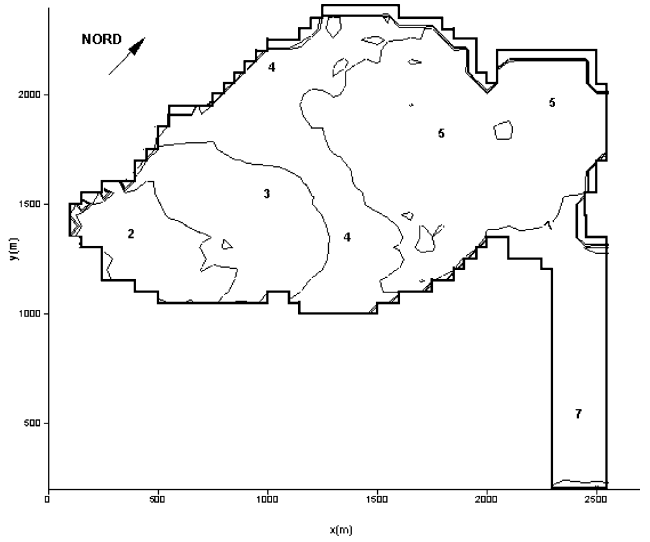

Fig. 15. Dissolved oxygen concentration field.

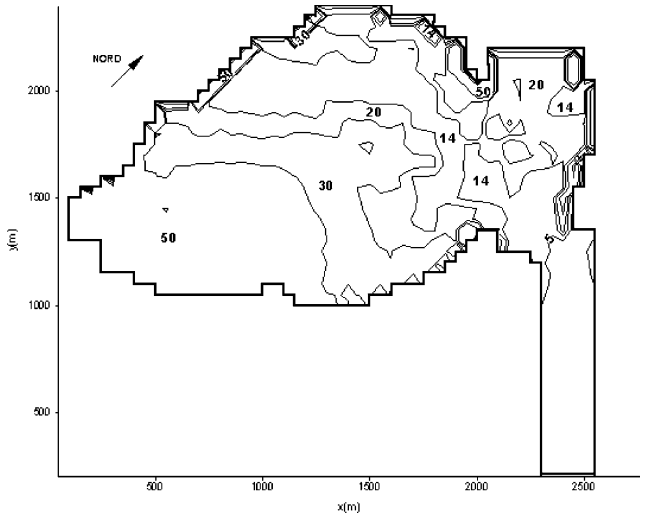

Fig. 16. Floating algae concentration field.

phate concentrations in the water column and the growth of the floating algae. In this region also lower values of dissolved oxygen can be observed (see Fig. 15).

The effect on the trophic lagoon behaviour of an higher rate of external phosphorous load, assumed equal to 20 times the actual (configuration b), can be inferred observing Fig. 18, in which the trend in time of the different species simulated concentration are reported. In the figure it is possible to observe that the complete replacement of the rooted plant with floating algae occurs

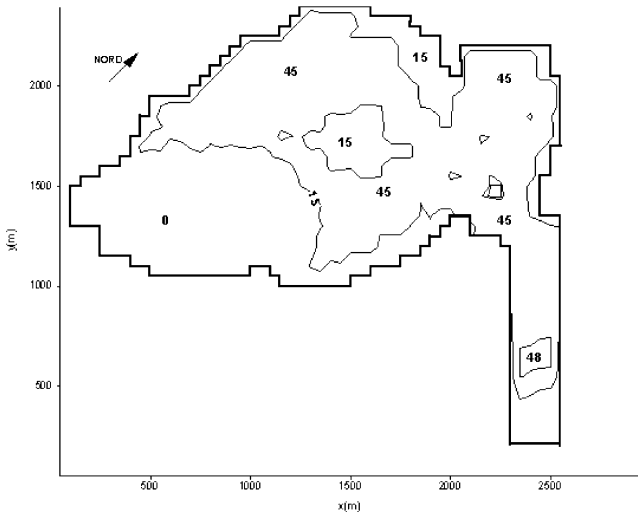

Fig. 17. *Zostera* concentration field.

in the first two-three years of simulation. This means that the higher the increment rate of external loads, the more rapidly the vegetal species substitution processes occur.

4. Discussion on the possible substitution mechanisms and consequence of such a substitution in terms of water anoxia vulnerability

The simulation results described in the previous paragraph allows us

- to advance a possible explanation on the mechanism driving the vegetal specie substitution from rooted plant to floating algae in a lagoon;
- to evidence that the main effect of the rooted plant substitution with floating algae is a major lagoon vulnerability process with regards to summer water anoxia.

The simulations have shown that

(a) the vegetal species substitution is a direct consequence of the increase of the nutrient external load discharged into the lagoon. The simulations have, in fact, shown that increasing the nutrient external load rate accelerates the substitution processes;
(b) the species substitution does not occur immediately after the nutrient load increase but with a delay corresponding to the time necessary to saturate the capability of sediments to accumulate adsorbed phosphorous;
(c) once the maximum capability to accumulate adsorbed phosphorus is reached in sediments, the substitution processes do not develop in progressive manner but rather through an evident discontinuity in time; practically, from a year to another the rooted plants are almost completely overcome by the floating species;

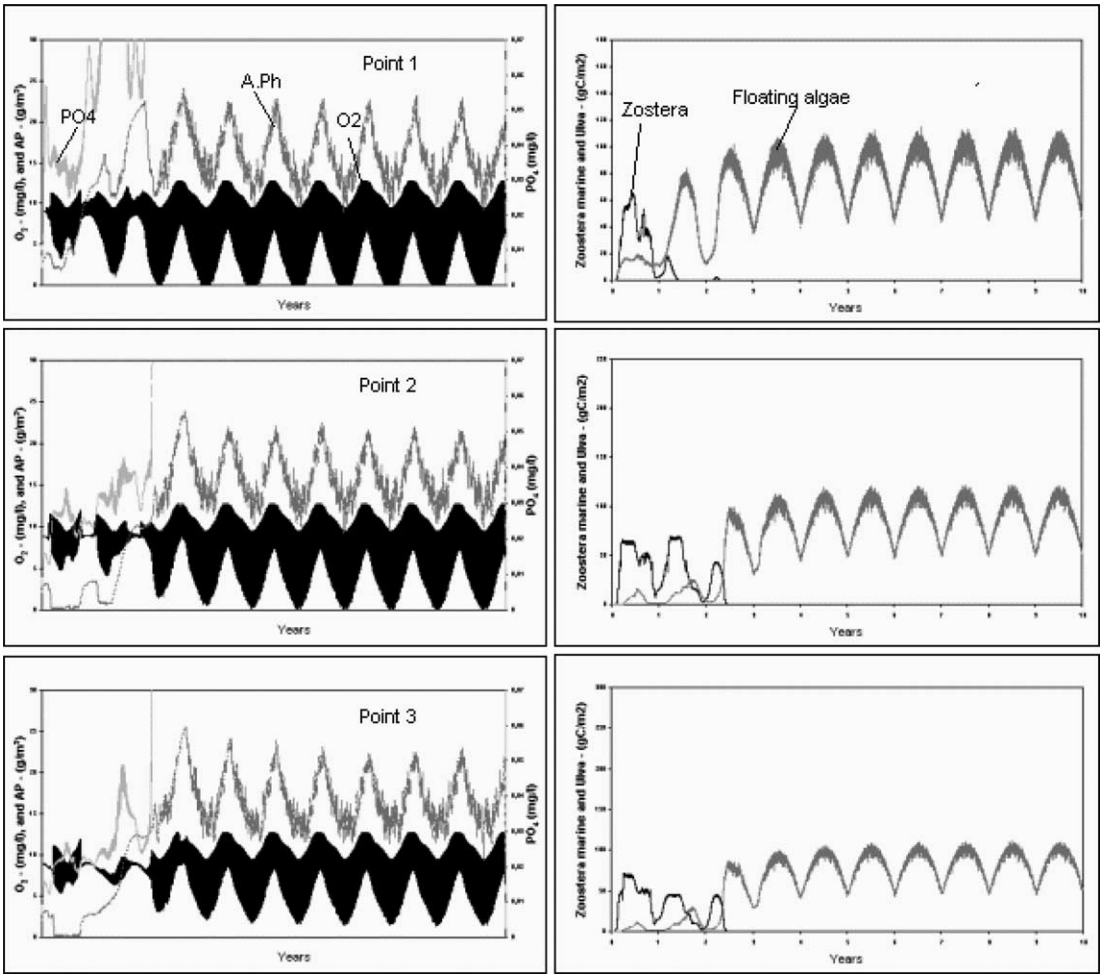

Fig. 18. (Left side) Dissolved oxygen, in the water column; orthophosphate concentration in the water column; adsorbed phosphorous into sediments. (Right side) *Zostera* concentration; floating species concentration.

(d) the vegetal species substitution does not occur simultaneously in each part of the lagoon, but it progressively extends to the entire lagoon starting from the regions far off the tidal channel;
(e) in the regions of the lagoon in which the floating species have become dominant the summer water anoxia risk appears considerably higher.

Points (a)–(c) highlight that the driving factor for a change of vegetal species is the increase in the quantity of phosphorous accumulated in the lagoon. When the flushing of phosphorus due to tidal flows, is not able to balance the external phosphorous loads, this nutrient accumulates in the lagoon.

At first, phosphorous accumulates in the sediments in form of adsorbed phosphorous; the good oxygenation conditions in the lagoon with low eutrophication level favour this processes.

Until the maximum quantity of phosphorus that can be adsorbed in the sediment solid phase is reached, the orthophosphate concentrations in the water column remain low and they constitute a limiting factor for the growth of floating algae. In such conditions, rooted plants are the dominant species in the lagoon because they uptake phosphorous, by enzymatic reactions, directly from sediments.

As a consequence, once the adsorbed phosphorous saturates the sediments, the dissolved phosphorous concentrations in the water column increase, allowing the growth of floating algae.

The growth in the upper layer of the water column of floating algae limits the growth of rooted plants as *Zostera*; the competition between the two different species does not seem to be relative to the nutrient up-take, it should rather be attributed to the effect of shadowing due to the presence of floating algae in the upper layers of the water column, which limits the light penetration in the deeper layers and thus inhibits the *Zostera* growth; a sufficient quantity of light needs to reach the bottom of the lagoon to prompt *Zostera* growth and it is thus evident how, in presence of floating algae, the light becomes the limiting factor for the *Zostera* growth.

The substitution of *Zostera* with floating algae is a quite fast process because another factor contributes to accelerate it. In the introduction it was underlined how the production of organic detritus is different for the two vegetal species, rooted and floating. In the case of rooted plants the organic detritus is produced at the end of the life cycle, in Autumn, when leaves fall down; while floating species have a more rapid turn-over and therefore the organic production is more uniform during the life cycle (from the end of winter to Autumn). Therefore, when the floating algae starts to have a concentration comparable with that of rooted plants, the cycles of organic matter, phosphorous and sulphur are completely altered. More organic detritus is produced by floating algae, and more organic detritus settles and accumulates into sediments from the end of winter to the critical summer season. This determines a major oxygen requirement for the mineralisation of organic matter and therefore more reducing conditions into sediments, which favour the phosphorous release in the water column and therefore the further growth of floating algae which, in turn, inhibits *Zostera* growth.

The above described sequence also explains why, once the species substitution has occurred, the lagoon presents a greater vulnerability to summer water anoxia: anoxic conditions into sediments, due to the higher organic detritus quantity accumulated, are more likely to be reached. As a consequence, hydrogen sulphide is produced by anaerobic mineralisation processes (sulphate reduction); this metabolite spreads in the water column and by re-oxidation accelerates the consumption of dissolved oxygen until it determines water anoxia in the entire water column.

In point (d) it was underlined that the vegetal species substitution does not occur simultaneously in each part of the lagoon, but it progressively extends to the entire lagoon starting from the regions far off the tidal channel. Specifically, the vegetal species substitution first occurs in the regions where the hydrodynamic influence of tidal flows is minor. These regions present low values of current velocity and, in absence of wind, low level of turbulent agitation. In these regions is, therefore, favoured the accumulation of phosphorous into sediments and in the water column and, as a consequence, the development of floating algae.

5. Conclusions

In this paper, the substitution mechanism of rooted aquatic plants (as for example *Zostera*) with floating species (as Ulva) in Mediterranean lagoons have been studied by using an eutrophication model. The simulations carried out for the specific case of Lagoon of Tortolì, Sardinia (Italy), have demonstrated the determinant role of the increase of the external phosphorous loads in the vegetal species selection and offered a possible explanation for the selection mechanism. The latter can be summarised as follows: once the maximum accumulation capability of adsorbed phosphorous in sediments is reached, the rate of phosphorous external loads produces an increment in the dissolved phosphorous present in the water column; such an increment favours the growth of floating species which inhibit, mainly due to light competition effect, the growth of rooted plants.

The simulations have shown that the substitution process is not progressive but it occurs abruptly. The dominance of floating algae has serious consequences on eutrophication processes and summer water anoxia vulnerability of the lagoon. This can be justified on the bases of the different production ways of organic detritus of floating algae with respect to rooted plants.

Certainly, the conclusions of this paper do not exhaust the matter concerning vegetal species selection in lagoons, because it is known that the selection also occurs among the floating species depending on the eutrophication level of the water body and a great variety of vegetal species can be found in lagoons.

Izzo and Signorini [1] have empirically shown that higher eutrophication levels favours vegetal species with a higher surface/volume ratio (it should be noted that rooted plants, as eelgrass or Ruppia, have a very low ratio). This seems to suggest that light competition is also, among the floating species, the main selection factor, because the photosynthetic activity is certain more efficient in the species with higher surface/volume, especially when the water turbidity is high as it occurs in highly eutrophical environments.

Because of the considerable complexity of the biological phenomena, the verification of such hypothesis requires more work in modelling the different vegetal species. Furthermore it can not excluded 'a priori' that others factors influence the vegetal species substitution: for example a different tolerance level of the species to some toxic substance as hydrogen sulphide, which develops in anoxic condition in the sediments.

However within these limits the simulations carried out reproduce the phenomena of substitution from rooted (as eelgrass) to floating vegetal species which has been observed in a great number of lagoons, and allow to provide a plausible explanation of the substitution mechanism.

Appendix A

Meaning of symbols and numerical values of the parameter used in the simulations

C_{max} =maximum *Zostera* concentration (gr C/l) = 100

D_{fs}; D_{sp}; D_{ds} =dispersion coefficient in sediments respectively of dissolved species, particulate organic carbon and dissolved organic carbon (m^2/s)=5×10^{-9}, 1×10^{-10}, 5×10^{-10}

D_{mo}; D_{mn} =molecular diffusion coefficient of dissolved oxygen and hydrogen sulphide (m/s)

$f_a(P_o)$ $=\frac{P_o}{k_{poa}+P_o}$ nutrient limiting factor in the water column

$f_s(P_o, P_a)$ $=\frac{P_o+P_a}{k_{pos}+P_o+P_a}$ nutrient limiting factor into the sediment

$f(O_2)$ $=\frac{O}{k_o+O}$ oxygen limiting factor

$f(C_d)$ $=\frac{C_d}{k_d+C_d}$ dissolved organic carbon limiting factor

$f_m(I)$ $=\frac{I}{I_m}\cdot \sin\left(\frac{\pi}{per}\cdot(t-t_s)\right)\cdot e^{-\gamma\cdot h}$ light limiting factor

$f_{al}(T)$ $=k_{tal}^{(T-T_{al})}, f_m(T)=\frac{T}{T_m}\cdot e^{\left(1-\frac{T}{T_m}\right)}, f_\mu(T)=k_{t\mu}^{(T-T_\mu)}$ temperature limiting factors

h_s =sediment layer thickness (cm) $= 6.0$

K_a =adsorbing–desorbing phosphorus rate in sediment (aerobic conditions) $(s^{-1}) = 2.5\times10^{-5}$

K_d =half saturation constant in dissolved organic carbon aerobic mineralisation (mg/l) $= 10$

$K_{d_{al}}$ =dissolved organic carbon production rate (from floating algae) $(s^{-1}) = 1\times10^{-7}$

K_{d_m} =dissolved organic carbon production rate (from *Zostera*) $(s^{-1}) = 1\times10^{-8}$

K_H =re-oxidation rate of hydrogen sulphide $(s^{-1}) = 4.2\times10^{-6}$

K_o =half saturation constant in dissolved oxygen limiting aerobic mineralisation (mg/l) $= 0.3$

K_{pmc}, K_{p_c} $=(\text{mg/l } PO_4^-)/(\text{mg/l } C_m), (\text{mg/l } PO_4^-)/(\text{mg/l } C_{al}) = 1\%$

K_p =rate of transformation particulate organic in dissolved organic carbon $(s^{-1}) = 5\times10^{-7}$

$K_{p_{al}}$ =particulate organic carbon production rate (from floating algae 'Ulva') $(s^{-1}) = 2.5\times10^{-8}$

K_{p_m} =particulate organic carbon production rate (from *Zostera*) $(s^{-1}) = 1.0\times10^{-8}$

K_{po} =half saturation constant for adsorbed and dissolved phosphorus at equilibrium (mg/l) $= 0.1$

K_{poa} =half saturation constant in phosphorus limiting floating algae growth (mg/l) $= 0.1$

K_{pos} =half saturation constant in phosphorus limiting *Zostera* growth (mg/l) $= 0.1$

K_s =dissolved organic carbon production rate in anaerobic conditions $(s^{-1}) = 2.5\times10^{-7}$

$K_{\gamma1}$; $K_{\gamma2}$; $K_{\gamma3}$ =extinction light coefficient $= 0.6$–0.1–0.1

P_{max} =maximum adsorbed phosphorus concentration in sediments (mg/l) $= 700$

p_{or} =porosity $= 0.8$

r_{al} =floating algae 'Ulva' respiration rate $(s^{-1}) = 0.25\times10^{-6}$

r_m =*Zostera* respiration rate $(s^{-1}) = 0.25\times 10^{-5}$

α_p =adsorbed phosphorus release rate in sediments in anaerobic conditions (mgP/ls) $= 5\times10^{-4}$

β_1; β_2; β_3; β_4 =stochiometric constant

μ_{cral} =floating algae 'Ulva' growth rate $(s^{-1}) = 5\times10^{-5}$

μ_{crm} =*Zostera* growth rate $(s^{-1}) = 0.5\times10^{-4}$

μ_d =aerobic mineralisation rate $(s^{-1}) = 1.2\times 10^{-3}$

v_s =settling velocity of particulate organic carbon (m/s) $= 3.5\times10^{-6}$

References

[1] G. Izzo, A. Signorini, Sviluppo di un metodo generale per la valutazione della qualitá ecologica di un ecosistema lagunare, Atti del XI Congresso Nazionale della Societá Italiana di Ecologia, 2001.

[2] H.K. Bach, A dynamic model describing the seasonal variations in growth and the distribution of eelgrass (*Zostera marina* L.), I, Model Theory Ecol. Model. 65 (1993) 31–50.
[3] S.L. Nielsen, K. Sand-Jensen, U. Borum, O. Geertz-Hansen, Depth colonization of eelgrass (*Zostera marina*), and Macroalgae as determined by water transparency in Danish coastal waters, Estuaries 25 (5) (2002) 1025–1032.
[4] A. Van Berk, H. Oostinga, North lake of tunis and its shores: Restoration and development, Terra et Aqua (49) (1992) 23–34.
[5] Pavoni B, Marcomini A, Sfriso A, Donazzolo R, Orio AA. Change in a estuarine ecosystem: The Lagoon of Venice as a case study, American Chemical Society, 1992 (Chapter 14).
[6] A. Sfriso, Decremento di produzione e cambio nella vegetazione macroalgale nella laguna di Venezia, Inquinamento 5 (1996) 80–88.
[7] A. Sfriso, F. Cavolo, La situazione delle alghe nella laguna di Venezia- Ambiente, Risorse e Salute- Giugno-Luglio, 1983.
[8] A. Sfriso, Flora and vertical distribution of macroalgae in the Lagoon of Venice: a comparison with previous studies, G. Bot. Ital. 121 (1987) 69–85.
[9] A. Sfriso, B. Pavoni, A. Marcomini, Macroalgae and phytoplancton standing crops in the central Venice Lagoon: primary production and nutrient balance, Sci. Total. Environ. 80 (1989) 139–159;
A. Sfriso, A. Marcomini, B. Pavoni, Relationship between macroalgal biomass and nutrient concentrations in a hypertrophic area of the Venice lagoon, Mar. Environ. Res. 22 (1987) 297–312.
[10] H. Brix, J.E. Lyngby, Uptake and translocation of phosphorus in eelgrass (*Zostera marina*), Mar. Biol. 90 (1985) 111–116.
[11] H. Iizumi, A. Hattori, Growth and organic production of eelgrass *Zostera marina* beds, Mar. Biol. 66 (1982) 59–65.
[12] C.P. MC Roy, R.J. Barsdate, Phosphate adsorption in eelgrass, Limnol. Oceanogr. 15 (1970) 6–13.
[13] J.L. Perez-Llorens, F.X. Niell, Short-term phosphate uptake kinetics in Zostera noltii Hornem: a comparison between excised leaves and sediment-rooted plants, Hydrobiologia 297 (1995) 17, 27.
[14] F. Cioffi, F. Gallerano, Management strategies for the control of eutrophication processes in Fogliano lagoon (Italy): a long-term analysis using a mathematical model, Appl. Math. Model. 25 (2001) 385–426.
[15] J.R. Hunter, C.J. Hearn, Lateral and vertical variation in wind-driven circulation in long, shallow lakes, J. Geophys. Res. 92 (1987) 13, 106–113,114.
[16] C. Koutitas, B. O'Connor, Modelling three-dimensional wind-induced flows, J. Hydraul. Div. 106 (1980).
[17] S. Komori, H. Ueda, F. Ogino, T. Mizushina, Turbulence structure and transport mechanism at the free surface in an open channel flow, Int. J. Heat Mass Transfer 25 (4) (1982) 513.
[18] Hydrocontrol—Misure dei principali parametri trofici e idrodinamici nella laguna di Tortolì— Rapporto interno, 2001.